Pergamon

Available online at www.sciencedirect.com

SCIENCE DIRECT®

Cement and Concrete Research 34 (2004) 2251–2260

CEMENT AND CONCRETE RESEARCH

Microscopic effects on chloride diffusivity of cement pastes—a scale-transition analysis

Peter Pivonka[a,*], Christian Hellmich[b], David Smith[a]

[a]Department of Civil and Environmental Engineering, School of Engineering, The University of Melbourne, Victoria 3010, Australia
[b]Institute for Strength of Materials, Vienna University of Technology, Karlsplatz, 13/202, A-1040 Vienna, Austria

Received 12 June 2003; accepted 2 April 2004

Abstract

For estimation of the durability of structures, it is highly desirable to quantify and simulate the chloride diffusion process in concrete. To this end, diffusion–cell experiments delivering the chloride diffusivity of cement pastes with different water–cement ratios (related to different microporosities) are evaluated in a scale-transition analysis. For prediction of the apparent chloride diffusivity, cement paste can be modelled by means of a differential homogenization scheme involving nondiffusive spherical inclusions in a diffusive matrix. As a result, chloride diffusivity of cement paste is obtained as a function of the microporosity and the chloride diffusivity in the micropore solution. Remarkably, the latter turns out to be one order of magnitude smaller than the chloride diffusivity in a pure salt solution system. The smaller diffusivity is probably caused by structuring of water molecules along the pore surface of cement paste.

Keywords: Chloride diffusion; Cement paste; Molecular water structuring; Scale transition; Multispecies transport

1. Introduction

One of the most severe durability problems in civil engineering is the deterioration of reinforced concrete structures through corrosion of the reinforcing steel. This process is accelerated by the possible presence of chloride which may be transported from the concrete surfaces (where it typically occurs as part of sea water or deicing salts on bridges) to the reinforcing steel. Thereby, chloride can be transported either together with water through the micropore space, driven by differences in the pore water pressure (advective transport), or chloride can diffuse through the pore water, driven by differences in the chloride concentration. Herein, we focus on the second form of transport. For estimation of the durability of structures, it is highly desirable to quantify and simulate this diffusion process. However, the chloride diffusivity through concrete and cement paste is characterized by a large variation, which depends strongly on the water–cement ratio [1–5]. Explanations for this large variation and its chemophysical origin are still a matter of debate. The possible significance of an electric (diffuse) double layer on the one hand [6–8], and of multispecies ionic transport on the other [9–11], have been discussed, but no commonly accepted view has been established so far.

In this paper, we want to contribute to an explanation for the variation and the magnitude of chloride diffusivity in cement pastes. We evaluate numerous experimental data from cell–diffusion tests published in the open literature [1–5,12,13], in the framework of a scale-transition analysis [14,15] between the micropore-space scale and the cement-paste scale.

2. Diffusion–cell experiments for determination of chloride diffusivity of cement pastes

Steady-state chloride diffusion through water-saturated concrete and cement pastes is usually described by Fick's first law [1–5,13,16], e.g., in the form [17]:

$$\mathbf{J}_{\text{paste}} = -\mathbf{D}_{\text{paste}} \cdot \nabla c_{\text{paste}}, \tag{1}$$

where $\mathbf{J}_{\text{paste}}$, $\mathbf{D}_{\text{paste}}$, and ∇c_{paste} are the molar flux, the second-order diffusivity tensor, and the concentration gra-

* Corresponding author. Tel.: +61-3-8344-4050; fax: +61-3-8344-4616.
E-mail addresses: Pivonka@civenv.unimelb.edu.au (P. Pivonka), Christian.Hellmich@tuwien.ac.at (C. Hellmich), David.Smith@unimelb.edu.au (D. Smith).
URL: http://www.fest.tuwien.ac.at.

0008-8846/$ – see front matter
doi:10.1016/j.cemconres.2004.04.010

dient of sodium chloride in cement paste. Cement paste can be considered as isotropic material, $\mathbf{D}_{\text{paste}} = \mathbf{1} D_{\text{paste}}$, with the diffusion coefficient D_{paste}, and the second-order unity tensor $\mathbf{1}$. D_{paste} is commonly determined by diffusion–cell tests, where two cells, filled with solutions characterized by different salt concentrations, are separated by a cylindrical cement-paste sample with cross-sectional area A_{sample} and thickness t_{sample} (Fig. 1a). The concentration in the upstream (source) compartment, $c_{\text{sol},1}$, is kept constant during the experiment. In addition, $c_{\text{sol},1}$ is chosen much larger than the salt concentration in the downstream (collector) compartment, $c_{\text{sol},2}$, i.e., $c_{\text{sol},1} >> c_{\text{sol},2}$. At the beginning of the test (see Fig. 1b), $c_{\text{sol},2}$ is chosen to be virtually zero. The chloride ions need a certain time span to move into the downstream compartment. The end of this time span is indicated by an increase of $c_{\text{sol},2}$ in the downstream compartment (see Fig. 1b). Monitoring $c_{\text{sol},2}$ over time allows for estimation of the chloride flux,

$$J_{\text{paste}} = \frac{V_{\text{cell},2}}{A_{\text{sample}}} \frac{\Delta c_{\text{paste},2}}{\Delta t} \tag{2}$$

where $V_{\text{cell},2}$ denotes the volume of the downstream cell. First, $\Delta c_{\text{sol},2}/\Delta t$ is changing (Fig. 1b), so that transient conditions prevail. The duration of transient conditions increases with increasing thickness of the specimen. Afterwards, steady-state conditions (i.e., $\Delta c_{\text{sol},2}/\Delta t = \text{const}$) are observed. They allow for estimation of the chloride diffusion coefficient, based on the discrete 1D specification of Fick's first law for the diffusion–cell test,

$$J_{\text{paste}} = -D_{\text{paste}} \cdot \frac{\Delta c_{\text{paste}}}{\Delta x} = -D_{\text{paste}} \cdot \frac{c_{\text{paste},2} - c_{\text{paste},1}}{t_{\text{sample}}} \tag{3}$$

D_{paste} can be expressed from Eq. (3) and Eq. (2), in the form:

$$D_{\text{paste}} = \frac{V_{\text{cell},2} \Delta c_{\text{paste},2}}{A_{\text{sample}} \Delta t} \frac{t_{\text{sample}}}{c_{\text{paste},1} - c_{\text{paste},2}}. \tag{4}$$

The chloride concentrations adjacent to the circular surfaces of the cement-paste sample, $c_{\text{paste},i}$, $i = 1, 2$, can be determined from the chloride concentrations in the solutions of the upstream and the downstream cell, $c_{\text{sol},i}$, $i = 1, 2$, and from the microporosity ϕ of the cement-paste sample, through

$$c_{\text{paste},i} = \phi \cdot c_{\text{sol},i} \qquad \text{with } i = 1, 2 \tag{5}$$

Insertion of Eq. (5) into Eq. (4) provides a relation for the determination of the diffusion coefficient of cement pastes from the physical properties accessible in diffusion–cell tests:

$$D_{\text{paste}} = \frac{V_{\text{cell},2} \Delta c_{\text{sol},2}}{A_{\text{sample}} \Delta t} \frac{t_{\text{sample}}}{c_{\text{sol},1} - c_{\text{sol},2}} \tag{6}$$

D_{paste} is commonly referred to as apparent (or cement paste) diffusion coefficient, or more properly, as mass transfer coefficient [17]. In the literature dealing with chloride diffusion through cement paste, this coefficient is also denoted as 'effective diffusion coefficient' of cement paste (see, e.g., Refs. [1,5,12]). However, in geo-environmental engineering, a distinction is made between the effective and the apparent diffusion coefficient (see Ref. [18] for details). In the following, to avoid any confusion, D_{paste} will be referred to as apparent diffusion coefficient of cement paste.

Diffusion–cell tests are typically performed to explore the effects of variations of (i) the water–cement ratio [1,5], (ii) the curing conditions [19,20], and (iii) the sodium chloride concentration [1,5] (Tables 1, 2, and 3 and Fig. 2).

Whereas the influence of different curing conditions and of the sodium chloride concentration turns out to be of

Table 1
Curing conditions of cement paste diffusion experiments (P81 [1], Y91 [2], N95 [3], TN92 [4], Mc95 [5], ACP01 [51], C01 [12], H95 [13])

Number	Description of curing condition
i	Air curing at room temperature (90–100% relative humidity)
ii	Immersed in saturated $Ca(OH)_2$ solution at room temperature
iii	Immersed in NaOH solution at room temperature
iv	Immersed in H_2O at room temperature

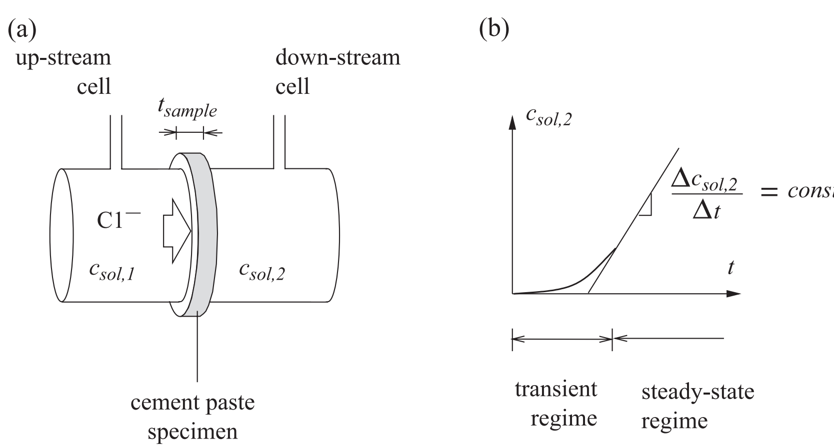

Fig. 1. Diffusion cell test: (a) schematical sketch; (b) time-dependent evolution of chloride concentration in downstream cell.

Table 2
Boundary conditions of cement-paste diffusion experiments (P81 [1], Y91 [2], N95 [3], TN92 [4], Mc95 [5], ACP01 [51], C01 [12], H95 [13])

Source	$c_{sol,1}$ [mol/l]	$c_{sol,2}$ [mol/l]	t_{cure} [days]	t_{test} [days]
P81	1 NaCl, $Ca(OH)_2$	$Ca(OH)_2$	60^{i}	21
Y91	1 NaCl, $Ca(OH)_2$	$Ca(OH)_2$	$90-270^{ii}$	21
N95	1 NaCl, 0.035 NaOH	0.035 NaOH	70^{v}	21
TN92	0.5 NaCl, $Ca(OH)_2$	$Ca(OH)_2$	90^{ii}	30
Mc95	0.5–4 NaCl	distilled H_2O	56^{i}	125
ACP01	1 NaCl, 0.035 NaOH	0.035 NaOH	84^{iii}	
C01	1 NaCl, $CaOH_2$	$Ca(OH)_2$	28^{iv}, 30^{ii}	21
H95	0.58 NaCl		60^{iv}	120

secondary importance, the strong functional dependence between water–cement ratio $(w/c)_i$ and apparent diffusion coefficient D_{paste} is striking (Fig. 2 and Table 3). The chemo-physical origin of this dependence will be elucidated next, by performance and interpretation of a scale-transition analysis.

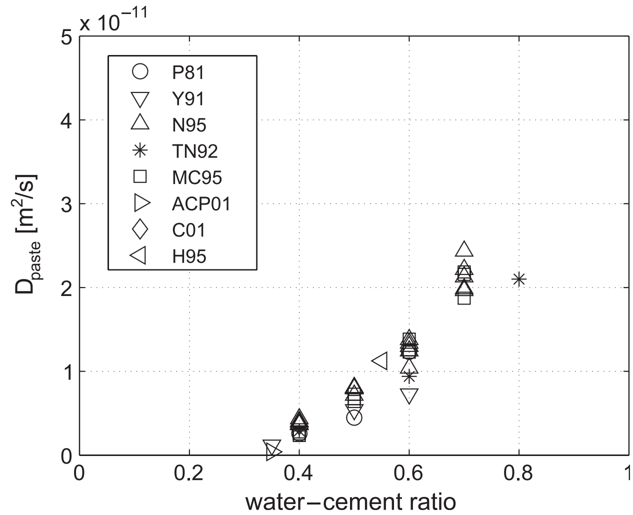

Fig. 2. Dependence of chloride diffusion coeffcients of cement pastes D_{paste} on w/c ratio (P81 [1], Y91 [2], N95 [3], TN92 [4], Mc95 [5], ACP01 [51], C01 [12], H95 [13]).

3. Evaluation of experiments by a scale-transition analysis

Diffusive transport of chloride (see Table 4 for ionic diameters) in a porous medium typically takes place in the pores of the material. For cement paste, different characteristic pore sizes motivate the distinction between micropores (‘capillary pores’ and ‘air pores’) on the one hand, and nanopores (‘gel pores’) on the other (Table 4). The rather large ratio of micropore diameter to the diameter of the ions encountered in cement paste (see Table 4) allows for a continuum description of diffusive transport of chloride through the (saturated) pores. In cement paste, the diffusive transport of chloride ions takes place in the micropores [21] as long as they percolate, i.e., as long as they form a continuous pathway [22]. This is the common situation to which we refer herein. However, in case the micropores close off, diffusive transport of ions is accomplished through the much smaller nanopores [22].

We consider cement paste as a porous medium defined on a representative volume element (RVE) of some millimeters characteristic length ℓ (Fig. 3).

This medium consists of two phases, schematically indicated in Fig. 3, a sodium-chloride-solution-filled micropore space and a solid phase consisting of alumino-silicate hydrates. While the solid phase is regarded as nondiffusive ($D_{solid} \equiv 0$), we assign an average diffusion coefficient $D_{poresol}$ to the pore fluid containing sodium chloride, presuming at this point the validity of Fick's first law in the micropore space

$$\boldsymbol{j}_{poresol} = -D_{poresol} \nabla c_{poresol} \tag{7}$$

This equation holds at the length scale which is considerably smaller than that of the micropores, d in Fig. 3, and which is, at the same time, significantly larger than that of the

Table 3
Experimental determination of composition and diffusivity of cement pastes: $(w/c)_i$ = initial water–cement ratio (before curing), given in the literature; $(w/c)_c$ = water–cement ratio after curing, $(w/c)_c \geq 0.42$; ϕ = solution-saturated porosity of cement paste; D_{paste} = apparent diffusion coefficient

Source	$(w/c)_i$ given	$(w/c)_c$ given (≥ 0.42)	ϕ Eq. (17)	D_{paste} [10^{-12} m²/s] given or Eq. (6)		
P81	0.40	0.42	0.065	2.600		
	0.50	0.50	0.157	4.470		
	0.60	0.60	0.249	12.35		
Y91	0.35	0.42	0.065	1.200		
	0.50	0.50	0.157	5.430		
	0.60	0.60	0.249	7.300		
N95	0.40	0.42	0.065	3.950		
	0.50	0.50	0.157	7.800		
	0.60	0.60	0.249	12.60		
	0.70	0.70	0.323	21.46		
TN92	0.40	0.42	0.065	2.900		
	0.60	0.60	0.249	9.400		
	0.80	0.80	0.384	21.00		
Mc95	0.40	0.42	0.065	2.353	2.549	2.784
	0.50	0.50	0.157	6.412	6.745	7.275
	0.60	0.60	0.249	12.29	12.57	13.84
	0.70	0.70	0.323	18.73	21.57	21.86
ACP01	0.35	0.42	0.065	0.40		
C01	0.40	0.42	0.065	3.646		
H95	0.55	0.55	0.206	11.25		

Table 4
Characteristic length scales of pores in cement paste and ions in solution

Pore type	ø Pores cement paste	Ion type	ø Ion unhydrated	ø Ion hydrated
Capillary	10 nm–100 μm [53]	Na^+	2 × 102 pm [41]	2 × 250–330 pm [45]
	< 1 μm [21]	K^+	2 × 138 pm [41]	2 × 180–200 pm [45]
Gel	< 10 nm [53]	Cl^-	2 × 181 pm [41]	2 × 200 pm [45]
	< 2 nm [21]	OH^-	2 × 25 pm [41]	2 × 30 pm [45]
Air	< 300 μm [53]	H_2O	–	0.28 nm [41]

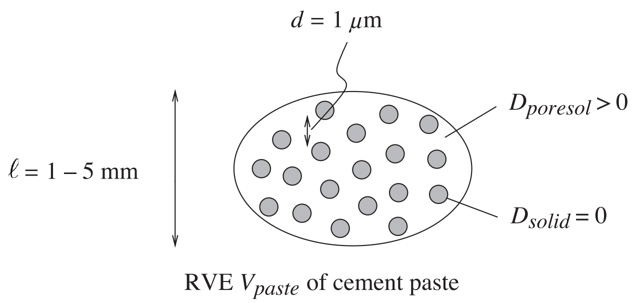

Fig. 3. Representation of cement paste as a two-phase material.

hydrated ions (see Table 4). At this scale, we are not aware of any measurement techniques for the estimation of $D_{poresol}$. As a first guess (the validity of which will be discussed later), $D_{poresol}$ may be assumed to match the sodium chloride diffusion coefficient of a pure solution system, i.e., $D_{poresol} = 1.61 \times 10^{-9}$ m^2/s [23] (see also Tables 5 and 6).

A micro–macro transition law relating $D_{poresol}$ and D_{paste} is standardly given in the form [15,24] (pp. 1268, Eq. (9))

$$\mathbf{D}_{paste} = \phi D_{poresol} \mathbf{T}, \tag{8}$$

where $\phi = V_{pore}/V_{paste}$ is the microporosity of cement paste (V_{pore} is the volume of micropores in the RVE with volume V_{paste}); and the second-order 'tortuosity tensor' $\mathbf{T}$, capturing geometrical information about the pore shape and arrangement (pore morphology). Accounting for the isotropy of the material, $\mathbf{D}_{paste} = \mathbf{1} D_{paste}$, Eq. (8) can be recast in the simpler from

$$D_{paste} = \phi D_{poresol} T \tag{9}$$

with the (dimensionless) tortuosity factor T. Alternatively, a (dimensionless) pore space topology factor (formation factor) $\bar{F} = 1/(\phi T)$ is commonly introduced [25], resulting in a micro–macro transition law of the form

$$D_{paste} = \frac{D_{poresol}}{\bar{F}} \tag{10}$$

Without any further knowledge about the pore space except its porosity ϕ and its isotropic nature, the tortuosity tensor $\mathbf{T}$ can be suitably estimated using the so-called differential scheme of continuum micromechanics [15,26,27]. Based on Eshelby's matrix inclusion problem [28], an infinitesimal amount of solid spherical inclusions is introduced into a matrix with $D_{poresol}$. The solid–fluid mixture is homogenized into a material with a well-defined diffusivity. This material serves as the matrix for the next infinitesimal amount of solid inclusions. This procedure is repeated until the actual solid volume fraction $(1-\phi)$ is reached, leading to the result [15]

$$\mathbf{T} = \phi^{1/2} \mathbf{1}, \tag{11}$$

$$\mathbf{D}_{paste} = \phi^{3/2} D_{poresol} \mathbf{1} \rightarrow D_{paste} = \phi^{3/2} D_{poresol} \tag{12}$$

Exactly the same result can be achieved by a differential effective medium approach for an assemblage of perfectly spherical grains [14], leading namely to $\bar{F} = \phi^{-3/2}$ in Eq. (10).

Having thus gained confidence in the relevance of the micro–macro transition law Eq. (12), we want to confront this relation to experimental data. This requires determination of the water-saturated microporosity ϕ from experiments.

Acker [29] has given the composition of cement pastes as a function of the water–cement ratio and the degree of hydration ξ (Fig. 4), reading as

$$\bar{V}_{cem}(\xi) = 1 - \xi \tag{13}$$

$$\bar{V}_{H_2O}(\xi) = \frac{\rho_{cem}}{\rho_{H_2O}} \langle w/c - 0.42\xi \rangle \tag{14}$$

$$\bar{V}_{hyd}(\xi) = \frac{\rho_{cem}}{\rho_{hyd}} \xi. \tag{15}$$

Here, $\langle \cdot \rangle$ represents the McAuley brackets, $\langle x \rangle = 1/2(x + |x|)$. $\rho_{cem} = 3.15$ kg/dm^3, $\rho_{H_2O} = 1.0$ kg/dm^3, and $\rho_{hyd} =$

Table 5
Salt diffusion (1:1 electrolytes, i.e., $z_+ = +1$, $z_- = -1$) and self-diffusion coefficients (infinite dilute solution, according to Ref. [23])

Electrolyte	D_{sol} [10^{-9} m^2/s]	D_+ [10^{-9} m^2/s]	D_- [10^{-9} m^2/s]
HCl	3.336	9.31	2.03
NaCl	1.610	1.33	2.03
KCl	1.994	1.96	2.03

Table 6
Salt diffusion coefficients at various concentrations at 25 °C (according to Ref. [23])

Concentration [mol/l]	D_{sol} [10^{-9} m^2/s]		
	NaCl	KCl	HCl
0.05	1.507	1.864	3.07
0.1	1.483	1.844	3.05
0.2	1.475	1.838	3.06
0.5	1.474	1.850	3.18
1.0	1.484	1.892	3.43
1.5	1.495	1.943	3.74
3.0	1.565	2.112	4.65

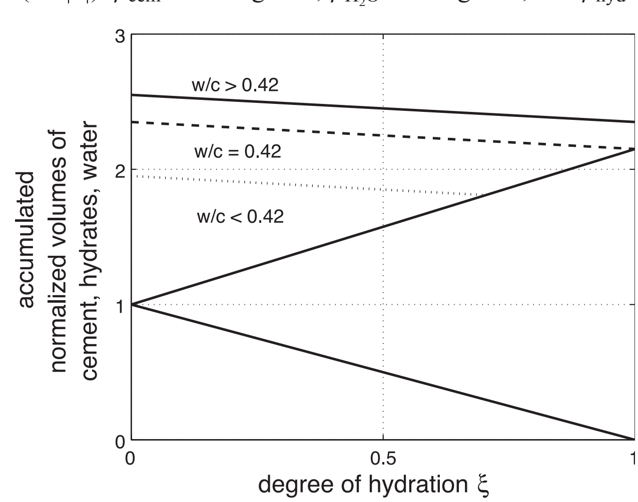

Fig. 4. Volumes of cement-paste components as a function of the degree of hydration, estimated according to Ref. [29].

1.46 kg/dm^3 [29] are the real mass densities of cement, water, and hydrates. $\bar{V}_i$ stands for the volume of component i normalized with respect to the volume of cement at $\xi = 0$ (i.e., at the beginning of the hydration);

$$\bar{V}_i = V_i / V_{\text{cem}}(\xi = 0) \rightarrow \bar{V}_{\text{cem}}(\xi = 0) = 1 \tag{16}$$

(see also Fig. 4).

For w/c < 0.42, lack of water causes part of the cement to remain unhydrated ($\xi_\infty < 1$; see dotted line in Fig. 4). However, all considered pastes with initial water–cement ratio $(\text{w/c})_\text{i} < 0.42$ (Fig. 4 and Table 2) were cured in water baths for at least 28 days (Table 2), so that they most probably attained a water–cement ratio of $(\text{w/c})_\text{c} = 0.42$ during curing. The duration of the curing period of all considered pastes, ranging between 28 and 270 days (Table 2), also suggests a complete hydration of the pastes at the end of the curing time, $\xi_\infty = 1$. Furthermore, water curing implies the filling of all original air pores (occupying normalized volume $\bar{V}_{\text{air}}$) with water. This renders the volume fraction of the water-saturated micropores (or porosity ϕ) as the following function of the water–cement ratio:

$$\phi(\text{w/c}) = \frac{\bar{V}_{\text{air}}(\xi = 1, \text{w/c} \geq 0.42) + \bar{V}_{\text{H}_2\text{O}}(\xi = 1, \text{w/c} \geq 0.42)}{[\bar{V}_{\text{air}} + \bar{V}_{\text{H}_2\text{O}} + \bar{V}_{\text{hyd}} + \bar{V}_{\text{cem}}](\xi = 1, \text{w/c} \geq 0.42)}, \tag{17}$$

where we make use of the relationships Eqs. (13)–(15). Respective porosity values for the data base depicted in Fig. 2 range between 7% and 38% (Table 3).

Experimentally determined data pairs (ϕ, D_{paste}; Table 3) are largely overestimated by the theoretical relationship Eq. (12) if $D_{\text{poresol}} = 1.61 \times 10^{-9}$ m^2/s is assumed (see Fig. 5); that is, the simple guess of setting the pore solution

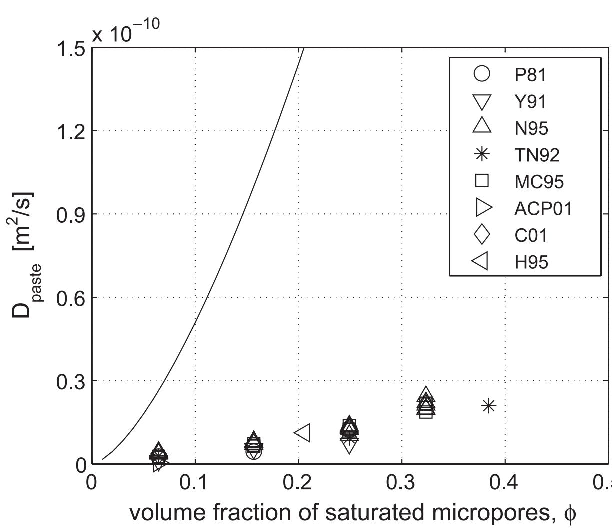

Fig. 5. Chloride diffusivity as a function of water-saturated porosity: comparison of experimental data (Table 3) and diffusion coefficients obtained by means of homogenization, Eq. (12) and $D_{\text{poresol}} = 1.61 \times 10^{-9}$ m^2/s.

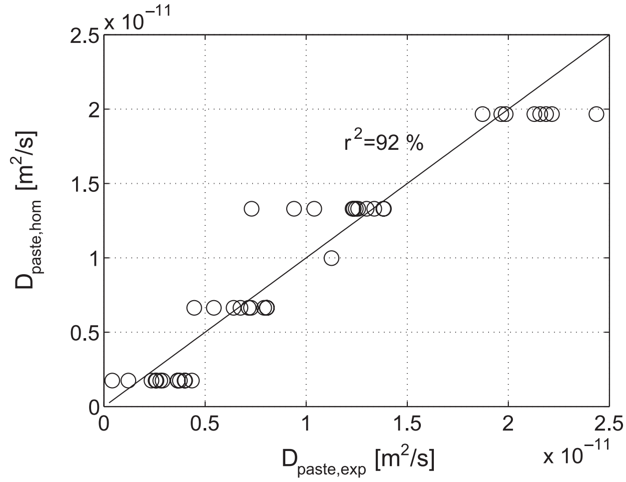

Fig. 6. Correlation of experimental data (Table 3) and diffusion coefficients obtained by means of homogenization, Eqs. (12) and (18).

diffusivity equal to the salt diffusivity in a pure solution system, $D_{\text{NaCl}} = 1.61 \times 10^{-9}$ m^2/s, turns out to be wrong.

However, what can also be seen is that the trend (shape) of the theoretical relationship fits very well with the one of the experiments. In fact, using a pore diffusion coefficient $D_{\text{poresol,opt}} = 1.07 \times 10^{-10}$ m^2/s, we get a high correlation coefficient of r^2=0.92 (Fig. 6), between D_{paste} and $D_{\text{paste,exp}}$. This is an extraordinary correlation given the simplicity of the micro–macro transition law and of the relation for the estimation of the water-saturated porosity Eq. (17). $D_{\text{poresol,opt}}$ was determined by minimizing the mean relative error between $n = 28$ experimental values $D_{\text{paste},i}$ (Table 3) and homogenization results $D_{\text{paste}}(\phi_i)$ from Eq. (12) (see Table 3 for the n values of ϕ_i)

$$\bar{e} = \frac{1}{n} \sum \frac{D_{\text{paste},i} - (\phi_i)^{3/2} D_{\text{poresol}}}{D_{\text{paste},i}} \rightarrow \text{Min} \Rightarrow D_{\text{poresol,opt}} \tag{18}$$

In other words, using this optimized diffusion coefficient to describe the diffusive transport in the pore solution of cement paste results in an excellent agreement between experimental data and values of the homogenized diffusion coefficients (see Fig. 7). It is noteworthy that models not formulated in the framework of micromechanics generally merge information on the pore morphology and on the transport properties into a single parameter (see, e.g., Refs. [30,31]). This parameter must then be repeatedly determined for different experiments, characterized by, e.g., different w/c values (porosity values) and different pore solution compositions. The choice of D_{poresol} for this parameter, i.e., substituting $\phi^{3/2}$ by ϕ in Eq. (12), implies assumption of straight transport pathways of ions through the pores. Respectively determined paste diffusivity may be classified as Voigt upper bounds. As a rule, they strongly overestimate experimentally obtained apparent diffusion coefficients.

The surprising result in Figs. 6 and 7 is that the various experimental data could be reproduced well using a single

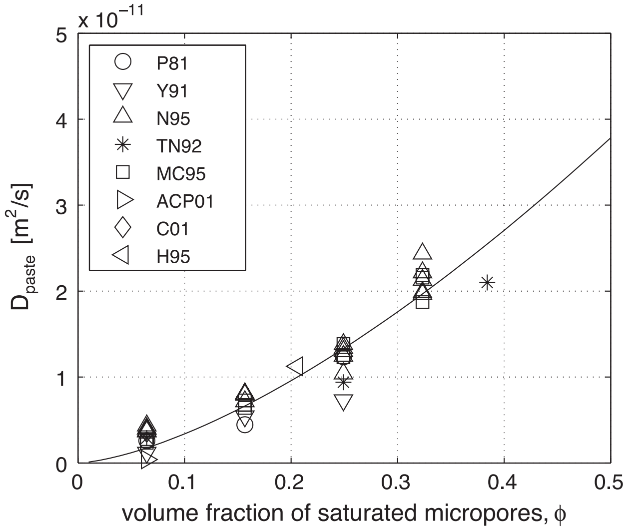

Fig. 7. Chloride diffusivity as a function of water-saturated porosity: comparison of experimental data (Table 3) and diffusion coefficients obtained by means of homogenization, Eqs. (12) and (18).

diffusion coefficient, i.e., $D_{\mathrm{poresol,opt}}$ of the pore solution. The question now raised is, why the pore diffusion coefficient, $D_{\mathrm{poresol,opt}}$, differs from the sodium chloride diffusion coefficient D_{NaCl} by a factor of 1/15. This question is addressed in the next section, but to this, some background understanding of multi-ion diffusion through a charged porous medium is first required.

4. Discussion of chloride diffusion in the micropore space of cement pastes

To suggest a reasonable explanation for the magnitude of the pore space diffusion coefficient $D_{\mathrm{poresol,opt}}$ we determined previously, we have to precisely define the physical meaning of the diffusion coefficients D_{paste} (Eq. (1)) and D_{poresol} (Eq. (7)). For this reason, we give a short review of diffusive transport in pure liquids and charged porous media.

In a system consisting exclusively of a solution (pure solution system), four types of diffusion are commonly distinguished [18] (see Fig. 8): (i) self-diffusion, (ii) tracer diffusion, (iii) salt diffusion, and (iv) counterdiffusion.

In case of dilute binary mixtures (one solute and one solvent), the first two types of diffusion (self-diffusion and tracer diffusion) can be described by Fick's first law [17]:

$$\mathbf{J}_i = -D_i \nabla c_i, \tag{19}$$

where $\mathbf{J}_i$ denotes the molar flux density, D_i is the diffusion coefficient of the ion, and c_i is the concentration of ionic species i. Self-diffusion coefficients for anions and cations in infinitely dilute solutions (Table 5) are computed from the Einstein relation, i.e., from $D_i = RTu_i$, where the experimental values for the mobility u_i are extrapolated to zero concentrations.

For the description of salt diffusion, i.e., diffusion of dilute binary electrolytes [two (charged) solutes and one solvent], the Nernst–Planck (N–P) equation is required [32], reading for individual ions as:

$$\mathbf{J}_i = -D_i\left(\nabla c_i + \frac{F}{RT} z_i c_i \nabla \psi\right), \tag{20}$$

where F is the Faraday constant, z_i and D_i are the charge number and the self-diffusion coefficient of the ith ion, R is the universal gas constant, T is the absolute temperature, and ψ is the electric potential. The N–P Eq. (20) expresses that the ionic species i may be driven by a gradient of the electric field $-\nabla\psi$ (migration) and/or by an ionic concentration gradient $-\nabla c_i$ (diffusion). In the absence of net current flow (electroneutrality), the gradient of the electric potential can be expressed as [32]:

$$\nabla\psi = -\frac{RT}{F}\frac{D_+ - D_-}{z_+ D_+ - z_- D_-}\frac{1}{c_{\mathrm{sol}}}\nabla c_{\mathrm{sol}}, \qquad c_{sol} = \frac{c_+}{v_+} = \frac{c_-}{v_-}, \tag{21}$$

where the subscripts +/− indicate cations and anions, respectively, and c_{sol} denotes the salt concentration. v_+ and v_- are the stoichiometric coefficients of the cations and anions. Integration of Eq. (21) leads the diffusion potential (liquid junction potential) for a binary electrolyte, reading as:

$$\Delta\psi_{\mathrm{L}} = -\frac{RT}{F}\frac{D_+ - D_-}{z_+ D_+ - z_- D_-}\ln\left(\frac{c_{\mathrm{sol},2}}{c_{\mathrm{sol},1}}\right). \tag{22}$$

Insertion of Eq. (21) into the N–P Eq. (20) delivers a steady-state diffusion equation for salts;

$$\mathbf{J}_{\mathrm{sol}} = -D_{\mathrm{sol}} \nabla c_{\mathrm{sol}}, \tag{23}$$

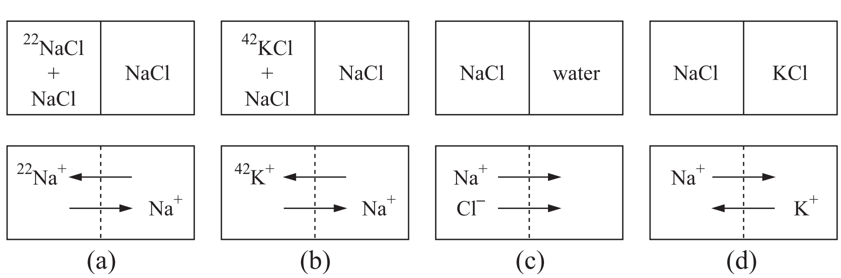

Fig. 8. Different types of diffusion: (a) self-diffusion, (b) tracer diffusion, (c) salt diffusion, and (d) counterdiffusion (according to Ref. [18]).

where $\mathbf{J}_{sol}$ and c_{sol} are the molar flux density and the concentration of the respective salt; and the salt diffusion coefficient D_{sol} has the form:

$$D_{sol} = \frac{D_+ D_- (z_+ - z_-)}{z_+ D_+ - z_- D_-} \tag{24}$$

(see Table 5). The mathematical similarity between Eq. (23) and Eq. (19) indicates that a salt solved in water behaves like a single ionic species, because of the electroneutrality requirement. In more detail, different self-diffusion coefficients of the anion and cation result in separation of the species. This leads to creation of a minute dipole density which then prevents further separation. The dipole density creates a potential (diffusion potential, Eq. (22)) which acts to speed up the ion with the smaller self-diffusion coefficients and slow down the ion with the larger self-diffusion coefficient.

Experiments show a dependence of salt diffusion coefficients on different concentrations (see Table 6). However, the diffusion coefficients of concentrated solutions (Table 6) and dilute solutions (Table 5) reasonably agree for concentrations up to 3.0 mol/l as far as NaCl and KCl solutions are concerned, and up to 1.0 mol/l for HCl solutions. Because we considered in our scale-transition analysis nondilute concentrations in the micropore solution which are smaller than 3 mol/l, (Table 2), the use of Fick's law Eq. (7) for the description of diffusive transport in the micropore space of cement paste is justified.

Still, with respect to pure solution systems, additional phenomena affect the diffusive transport in the micropores of cement, reducing the drift speed of chloride. The decrease of ionic drift speed in the pores may be attributed to (i) the presence of an (electrical) diffuse double layer (DDL) on particle surfaces, (ii) the presence of high concentrations of multiple ions in the pore solution, and (iii) changes of the viscosity of the pore solution caused by structuring of water. Let us more profoundly discuss these three possibilities:

(i) Zeta potential measurements of cement pastes [33,34] indicate negative surface charges on cement-paste particles. The region where 'counterions' balance this excess charge is generally called electrical DDL [25]. It may be described by double- or triple-layer models (see, e.g., Ref. [35]). However, the presence of a DDL has been shown to *increase* (rather than decrease) the salt diffusivity [25]. At low salinity and/or high cation exchange capacity, there is a large difference in permeability for counterions (Na) and co-ions (Cl), a phenomenon called permselectivity. For a charged porous material at low salinity, the permselectivity increases the (absolute) value of the diffusion potential until its upper bound, which corresponds to the potential of a perfect membrane. The membrane potential increases the velocity of the co-ions to avoid generation of electric current. It follows that the macroscopic diffusion coefficient is increased by this effect [25]. Consequently, the retardation of chloride ions cannot be attributed to the DDL. The DDL seemingly does not have a discernible effect on the chloride diffusivity of cement pastes at all, probably because of its compression due to salt concentrations around 1 mol/l NaCl, as was shown for platy clay soil [54].

(ii) Experimental investigations of the cement pore solution have shown that the pore solution consists of multiple ions, such as Na^+, K^+, Ca^{2+}, OH^-, and SO_4^{2-} ions [21,36–39]. While in this case, the ionic flux of each species can still be quantified by the N–P Eq. (20), the electric potential does not follow any more from Eq. (22), but from the more complex Henderson formula [40]

$$\Delta\psi_L = -\frac{RT}{F} \frac{\sum_{i=1}^{N} z_i D_i (c_{i,2} - c_{i,1})}{\sum_{i=1}^{N} z_i^2 D_i (c_{i,2} - c_{i,1})} \ln \left(\frac{\sum_{i=1}^{N} z_i^2 D_i c_{i,2}}{\sum_{i=1}^{N} z_i^2 D_i c_{i,1}} \right) \tag{25}$$

This formula allows for quantification of the effect of multiple ions on the chloride diffusivity, e.g., for a NaCl concentration ratio of $c_{sol,2}/c_{sol,1} = 1{:}10$, addition of ions, such as Na^+, K^+, and OH^- in concentrations 150, 400, and 550 mol/m^3 to a 1-mol NaCl solution, resulting in a multispecies solution typical for cement pastes [11], which leads to a decrease of the (absolute value of) the diffusion potential from $\psi_L = -12$ mV[1] (for the NaCl solution Eq. (22)) to $\psi_L = -3$ mV (for the multispecies solution Eq. (25)). This decrease and specification of the N–P Eq. (20) for chloride, $z_{Cl} = -1$, show that the presence of Na^+, K^+, and OH^- leads to an acceleration (rather than to a retardation) of the chloride drift speed. Hence, judging from the diffusion potential, the decrease of chloride diffusivity in the saturated micropore space of cement pastes cannot be attributed to the presence of multiple ionic species.

A second characteristic of multispecies solutions is the smaller distance between ions, increasing the importance of ion–ion interactions. The presence of high concentrations of multiple ions in solution is standardly taken into account using activity coefficients [41] which describe the deviation of a solution from ideality. There are several theories for describing the relationship between activity coefficient and ionic concentration (strength) of the solution. Among these, the Pitzer model [42] and the extended Debye–Hückel model [43] are most commonly applied. However, application of the latter model for salt concentrations up to 1 mol/l at the pure solution level showed only a small variation of the salt diffusion coefficient,

[1] The diffusion potential is chosen as zero at the upstream side of the sample.

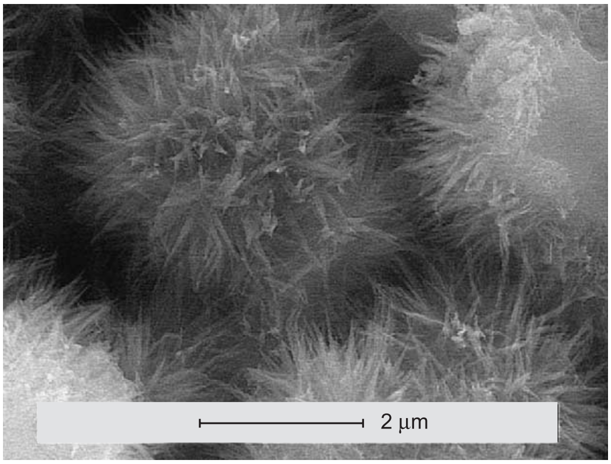

Fig. 9. Morphology of the cement-paste microstructure obtained from environmental scanning electron microscope (ESEM), 28 days after the onset of hydration (according to Ref. [52]).

typically between 4% (for NaCl and KCl solutions) and 8% (for LiCl solution, see Ref. [44] for details). Hence, the influence of additional ions in a multispecies solution seems inappropriate to explain the decrease of salt diffusivity in the micropores of cement pastes by the factor 1/15. This is in agreement with the numerical simulations of multispecies diffusion conducted in Ref. [11].

(iii) Evidence has been put forward for almost one century that charged surfaces may imply structuring or layering of water (see Ref. [45] for a historical review). This phenomenon is known to occur in numerous materials, including, e.g., biopolymers [46]. In more detail, the polar nature of the water molecules leads to their absorption at the charged surfaces, constituting a first layer. Then, additional layers adhere one upon the other, forming a multilayered network. This layered network has physical properties which are distinctively different from standard liquid water; that is, the viscosity of layered water is significantly higher. Molecular dynamic (MD) simulations of a clay–salt water system show that the salt diffusion coefficient strongly depends on the viscosity of the pore solution [47,48]. While a viscosity of $\mu_w = 0.001$ kg/(m s) leads to a diffusion coefficent of $D_{sol} \approx 1.7 \times 10^{-9}$ m^2/s, which is close to the one for a NaCl solution ($D_{sol} = 1.61 \times 10^{-9}$ m^2/s, see Table 5), an increase of viscosity to $\mu_w = 0.007$ kg/(m s) leads to a diffusion coefficient of $D_{sol} \approx 2.5 \times 10^{-10}$ m^2/s. The latter value is of the same order of magnitude as the chloride diffusivity we determined for the pore solution of cement paste ($D_{poresol,opt} = 1.1 \times 10^{-10}$ m^2/s). The viscosity increase (and the diffusivity decrease, respectively) can be detected over a distance as large as several hundred nanometers [49]. The 'spiney structure' of cement paste at complete hydration (Fig. 9) [50] exhibits features of exactly this characteristic length. This renders structuring of water as the prime candidate for the explanation of the decrease of chloride diffusivity in the micropore space of cement paste with respect to a pure salt solution.

5. Conclusions

For prediction of the apparent chloride diffusivity, cement paste can be modelled by means of a differential homogenization scheme involving nondiffusive spherical inclusions in a diffusive matrix. As a result, chloride diffusivity of cement paste is obtained as a function of the microporosity and the chloride diffusivity in the micropore solution. Remarkably, the latter turns out to be one order of magnitude smaller than the chloride diffusivity in a pure salt solution system. The smaller diffusivity is probably caused by a higher viscosity of the pore solution. This higher viscosity can be explained by the structuring of water molecules along the charged pore surfaces, a well-known phenomenon in clays and biological materials.

Acknowledgements

The first author gratefully acknowledge the financial support of this study by the 'Austrian Foundation for the Promotion of Scientific Research (FWF)' in the course of an Erwin Schrödinger scholarship.

Appendix A. Notation

The following notation is used in this paper

A_{sample}	Area of cement-paste sample [m^2]
c_i	Concentration of ions in pure solution [mol/m^3]
c_{sol}	Sodium chloride ion concentration [mol/m^3]
$c_{sol,1}$, $c_{sol,2}$	Sodium chloride ion concentration in upstream and downstream compartment [mol/m^3]
c_{paste}	Sodium chloride ion concentration in cement paste [mol/m^3]
$c_{poresol}$	Sodium chloride ion concentration in pore solution of cement paste [mol/m^3]
d	Characteristic pore size [m]
D_i	Self-diffusion coefficient of ion i [m^2/s]
D_{sol}	Salt diffusion coefficient [m^2/s]
D_{solid}	Sodium chloride ion diffusion coefficient of solid phase of cement paste [m^2/s]
D_{paste}	Sodium chloride ion diffusion coefficient in cement paste [m^2/s]
$D_{paste,exp}$	Experimentally determined sodium chloride ion diffusion coefficient in cement paste [m^2/s]
$D_{poresol}$	Sodium chloride ion diffusion coefficient in pore solution of cement paste [m^2/s]
$D_{poresol,opt}$	Sodium chloride ion diffusion coefficient in pore solution of cement paste obtained from optimization analysis [m^2/s]
D_{NaCl}	Sodium chloride diffusion coefficient [m^2/s]
$\mathbf{D}_{paste,hom}$	Homogenized paste diffusion coefficient [m^2/s]
$\bar{e}$	Relative error between homogenized and experimental diffusion coefficients

Appendix A (*continued*)

F	Faraday constant $F = 96{,}500$ [C/mol]
$\bar{F}$	Formation factor [–]
$\mathbf{j}_{\mathrm{poresol}}$	Sodium chloride molar mass flux density in pore solution of cement paste [mol/(m^{3}s)]
$\mathbf{J}_i$	Molar mass flux density of the ith ion [mol/(m^{3}s)]
$\mathbf{J}_{\mathrm{sol}}$	Sodium chloride molar mass flux density in pure solution [mol/(m^{3}s)]
$\mathbf{J}_{\mathrm{paste}}$	Sodium chloride molar mass flux in cement paste [mol/(m^{3}s)]
ℓ	Characteristic length of representative volume element [m]
n	Number of experimental values of apparent diffusion coefficients
R	Universal gas constant $R = 8.31$ [J/(K mol)]
t_{sample}	Thickness of cement-paste sample [m]
Δt	Time increment for diffusive transport [s]
T	Absolute temperature [K]
T, $\mathbf{T}$	Tortuosity factor, tortuosity tensor [–]
u_i	Ion mobility [(m^2 mol)/(J s)]
w/c	Water–cement ratio [–]
$(\mathrm{w/c})_{\mathrm{i}}$	Water–cement ratio before curing [–]
$(\mathrm{w/c})_{\mathrm{c}}$	Water–cement ratio after curing [–]
$(\mathrm{w/c})_{\mathrm{exp}}$	Experimental water–cement ratio [–]
V_{paste}	Volume of cement paste [m^3]
$\bar{V}_{\mathrm{air}}$	Volume of air pores normalized with respect to volume of cement at $\xi = 0$ [–]
$\bar{V}_{\mathrm{H_2O}}$	Volume of water normalized with respect to volume of cement at $\xi = 0$ [–]
$\bar{V}_{\mathrm{hyd}}$	Volume of hydrates normalized with respect to volume of cement at $\xi = 0$ [–]
$\bar{V}_{\mathrm{cem}}$	Volume of cement normalized with respect to volume of cement at $\xi = 0$ [–]
Δx	Space increment for diffusive transport (x-direction) [m]
z_i	Charge number of the ith ion [–]
v_+, v_-	Stoichometric coefficients of cations and anions [–]
ξ	Degree of hydration [–]
ρ_{cem}	Mass density of cement [kg/m^3]
ρ_{hyd}	Mass density of hydrates [kg/m^3]
$\rho_{\mathrm{H_2O}}$	Mass density of water [kg/m^3]
ϕ	Capillary porosity of cement paste [–]
ϕ_{exp}	Experimental capillary porosity of cement paste [–]
$\phi_{\mathrm{exp},i}$	Experimental capillary porosity of ith experiment [–]
ψ	Electric potential [V]
$\Delta\psi_{\mathrm{L}}$	Diffusion potential [V]

References

[1] C. Page, N. Short, A. Tarras, Diffusion of chloride ions in hardened cement pastes, Cem. Concr. Res. 11 (3) (1981) 395–406.

[2] S. Yu, C. Page, Diffusion in cementitious materials: 1. Comparative study of chloride and oxygen diffusion in hydrated cement pastes, Cem. Concr. Res. 21 (1991) 581–588.

[3] V. Ngala, C. Page, L. Parrott, S. Yu, Diffusion in cementitious materials: 2. Further investigations of chloride and oxygen diffusion in well-cured OPC and OPC/20% PFA pastes, Cem. Concr. Res. 25 (4) (1995) 819–826.

[4] L. Tang, L.-O. Nilson, Rapid determination of chloride diffusivity in concrete by applying an electrical field, ACI Mater. J. 89 (1) (1992) 49–53.

[5] K. MacDonald, D. Northwood, Experimental measurements of chloride ion diffusion rates using a two-compartment diffusion cell: effects of material and test variables, Cem. Concr. Res. 25 (7) (1995) 1407–1416.

[6] T. Zhang, O.E. Gjørv, Effect of ionic interaction in migration testing of chloride diffusivity in concrete, Cem. Concr. Res. 25 (7) (1995) 1535–1542.

[7] J.-Z. Zhang, N. Buenfeld, Presence and possible implications of a membrane potential in concrete exposed to chloride solution, Cem. Concr. Res. 27 (6) (1997) 853–859.

[8] S. Chatterji, Colloid electrochemistry of saturated cement paste and some properties of cement based materials, Adv. Cem. Based Mater. 7 (1998) 102–108.

[9] E. Samson, G. Lemaire, J. Marchand, J. Beaudoin, Modeling chemical activity effects in strong ionic solutions, Comput. Mater. Sci. 15 (1999) 285–294.

[10] E. Samson, J. Marchand, Numerical solution of the extended Nernst–Planck model, J. Colloid Interface Sci. 215 (1999) 1–8.

[11] O. Truc, J. Ollivier, L. Nielsson, Numerical simulation of multi-species transport through saturated concrete during migration test—MsDiff code, Cem. Concr. Res. 30 (2000) 1581–1592.

[12] M. Castellote, C. Alonso, C. Andrade, G. Chadbourn, C. Page, Oxygen and chloride diffusion in cement pastes as a validation of chloride diffusion coefficients obtained by steady-state migration tests, Cem. Concr. Res. 31 (2001) 621–625.

[13] H. Hornain, J. Marchand, V. Duhot, M. Moranville-Regourd, Diffusion of chloride ions in limestone filler blended cement pastes and mortars, Cem. Concr. Res. 25 (8) (1995) 1667–1678.

[14] P. Sen, C. Scala, M. Cohen, A self-similar model for sedimentary rocks with application to the dielectric constant of fused glass beads, Geophysics 46 (5) (1981) 781–795.

[15] L. Dormieux, E. Lemarchand, Homogenization approach of advection and diffusion in cracked porous media, ASCE J. Eng. Mech. 127 (12) (2001) 1267–1274.

[16] M. Castellote, C. Andrade, C. Alonso, Measurement of steady and non-steady-state chloride diffusion coefficients in a migration test by means of monitoring the conductivity in the anolyte chamber. Comparison with natural diffusion tests, Cem. Concr. Res. 31 (10) (2001) 1411–1420.

[17] E. Cussler, Diffusion Mass Transfer in Fluid Systems, 2nd edition, Cambridge Univ. Press, New York, USA, 1997.

[18] C. Shackelford, D. Daniel, Diffusion in saturated soil: I. Background, Geotech. Eng. 117 (3) (1991) 467–484.

[19] C. Dehghanian, M. Arjemandi, Influence of slag blended cement concrete on chloride diffusion rate, Cem. Concr. Res. 27 (6) (1997) 937–945.

[20] K. Ampadu, K. Torii, M. Kawamura, Beneficial effect of fly ash on chloride diffusivity of hardened cement paste, Cem. Concr. Res. 29 (1999) 585–590.

[21] N. Buenfeld, G. Glass, A. Hassanein, J.-Z. Zhang, Chloride transport in concrete subjected to electric field, ASCE J. Mater. Civ. Eng. 10 (4) (1998) 220–228.

[22] E. Garboczi, D. Bentz, Computer simulation of the diffusivity of cement based materials, J. Mater. Sci. 27 (1992) 2083–2092.

[23] R. Robinson, R. Stokes, Electrolyte Solutions, 2nd edition, Butterworths, London, England, 1959.

[24] J. Bear, Y. Bachmat, Introduction to Modelling of Transport Phenomena in Porous Media, vol. 4, Kluwer Academic Publishing, Dordrecht, Netherlands, 1991.

[25] A. Revil, Ionic diffusivity, electrical conductivity, membrane and thermoelectric potentials in colloids and granular porous media: a unified model, J. Colloid Interface Sci. 212 (1999) 503–522.

[26] A. Zaoui, Structural morphology and constitutive behavior of microheterogeneous materials, in: P. Suquet (Ed.), Continuum Micromechanics, CISM courses and lectures No. 377, International Centre for Mechanical Science, Springer, New York, USA, 1997, pp. 291–347.

[27] E. Lemarchand, Contribution de la microméchanique ál'étude des phénoménes de transport et couplage poromechanique dans les milieux poreux: Application aux phenomenes de gonflement dans les géomatériaux, Ph.D. thesis, Ecole Nationale des Ponts et Chaussées, Paris, France, 2001.

[28] J.D. Eshelby, The determination of the elastic field of an ellipsoidal inclusion, and related problems, Proc. R. Soc. Lond., A 241 (1226) (1957) 376–396.

[29] P. Acker, Micromechanical analysis of creep and shrinkage mechanisms, in: F.-J. Ulm, Z. Bažant, F. Wittmann (Eds.), Creep, Shrinkage, and Durability of concrete and other Quasi-brittle Material—Proceedings of the Sixth International Conference CONCREEP-6@MIT, Elsevier, Amsterdam, 2001, pp. 15–26.

[30] L. Tang, Concentration dependence of diffusion and migration of chloride ions: Part 1. Theoretical considerations, Cem. Concr. Res. 29 (1999) 1463–1468.

[31] G. Glass, N. Buenfeld, Theoretical assessment of steady state diffusion cell test, J. Mater. Sci. 33 (1998) 5111–5118.

[32] J. Newman, Electrochemical Systems, 2nd edition, Prentice-Hall, Englewood Cliffs, NJ, USA, 1991.

[33] E. Nägele, The zeta potential of cement, Cem. Concr. Res. 15 (3) (1985) 453–462.

[34] E. Nägele, The transient zeta potential of hydrating cement, Chem. Eng. Sci. 44 (8) (1989) 1637–1645.

[35] P. Hiemenz, R. Rajagopalan, Principles of Colloid and Surface Chemistry, 3rd edition, Marcel Dekker, New York, USA, 1997.

[36] S. Diamond, Effects of two Danish fly ashes on alkali contents of pore solutions of cement–fly ash pastes, Cem. Concr. Res. 11 (1981) 383–394.

[37] C. Andrade, Calculation of chloride diffusion coefficients in concrete from ionic migration measurements, Cem. Concr. Res. 23 (1993) 724–742.

[38] T. Zhang, O.E. Gjørv, An electrochemical method for accelerated testing of chloride diffusivity of concrete, Cem. Concr. Res. 24 (8) (1994) 1534–1548.

[39] S. Chatterji, Evidence of variable diffusivity of ions in saturated cementitious materials, Cem. Concr. Res. 29 (1999) 995–998.

[40] F. Helfferich, Ion Exchange, McGraw-Hill, New York, USA, 1962 (series in Advanced Chemistry).

[41] P. Atkins, J. de Paula, Atkins' Physical Chemistry, 7th edition, Oxford Univ. Press, New York, USA, 2002.

[42] K. Pitzer, Thermodynamics of electrolytes: I. Theoretical basis and general equations, J. Phys. Chem. 77 (2) (1973) 268–277.

[43] U. Kunze, Grundlagen der quantitativen Analyse, 2nd edition, Georg Thieme, Stuttgart, Germany, 1986.

[44] L. Tang, Concentration dependence of diffusion and migration of chloride ions: Part 2. Experimental evaluations, Cem. Concr. Res. 29 (1999) 1469–1474.

[45] G. Pollack, Cells, Gels and the Engines of Life: A New Unifying Approach to Cell Function, Ebner and Sons, Seattle, WA, USA, 2001.

[46] J. Israellachvili, H. Wennerström, Role of hydration and water structure in biological and colloidal interactions, Nature 379 (1996) 219–225.

[47] Y. Ichikawa, K. Kawamura, M. Nakano, K. Kitayama, N. Fujii, Molecular behavior and micro/macro analysis of diffusion problem in bentonite, CDROM Proceedings of the European Congress on Computational Methods in Applied Sciences and Engineering, Barcelona, Spain, 2000.

[48] Y. Ichikawa, K. Kawamura, N. Fujii, T. Nattavut, Molecular dynamics and multiscale homogenization analysis of seepage/diffusion problem in bentonite clay, Int. J. Numer. Methods Eng. 54 (2002) 1717–1749.

[49] A. Szent-Györgyy, The Living State. With Observations of Cancer, Academic Press, New York, USA, 2001.

[50] M. Ashby, D. Jones, Engineering Materials, vol. 2, Elsevier, New York, USA, 1994.

[51] A. Asbridge, G. Chadbourn, C. Page, Effects of metakaolin and the interfacial transition zone on the diffusion of chloride ions through cement mortars, Cem. Concr. Res. 31 (2001) 1567–1572.

[52] J. Tritthart, F. Häußler, Pore solution analysis of cement pastes and nanostructural investigations of hydrated C_3S, Cem. Concr. Res. 33 (2003) 1063–1070.

[53] J. Stark, B. Wicht, Dauerhaftigkeit von Beton, 2nd edition, Birkhäuser, Basel, Schweiz, 2001.

[54] D. Smith, P. Pivonka, C. Jungnickel, S. Fiytus, Theoretical analysis of anion exclusion and diffusive transport through platy-clay soils, Trans. Porous Media 55 (2004) 1–27.